Delineation of the Mechanisms of Tendon Gliding Resistance Within the Carpal Tunnel

Anika Filius, MD, Ph.D.[a,b,c], **Andrew R. Thoreson, MSc**[a], **Yasuhiro Ozasa, MD PhD**[a], **Kai-Nan An, PhD**[a], **Chunfeng Zhao, MD**[a], and **Peter C. Amadio, MD**[a]

[a]Biomechanics Laboratory, Division of Orthopedic Research, Department of Orthopedic Surgery, Mayo Clinic, 200 1st Street SW, Rochester, Minnesota, USA [b]Department of Plastic and Reconstructive Surgery and Hand Surgery, Erasmus MC, University Medical Centre Rotterdam, The Netherlands [c]Department of Rehabilitation Medicine, Erasmus MC

Abstract

Background—Forceful, high-velocity, and repetitive manual hand tasks contribute to the onset of carpal tunnel syndrome. This study aimed to isolate and identify mechanisms that contribute to tendon gliding resistance in the carpal tunnel.

Methods—Eight human cadaver hands (four pairs) were used. Tendon gliding resistance (force, energy, and stiffness) was measured under different conditions: with intact and with divided subsynovial connective tissue, at 2 mm/s and 60 mm/s tendon excursion velocity, and with and without relaxation time before tendon excursion.

Results—Subsynovial connective tissue stretching substantially contributed to increased gliding resistance force and energy during higher tendon excursion velocities, and subsynovial connective tissue stiffening was observed. Poroelastic properties of the tendon (and possibly the subsynovial connective tissue) also appear to be involved because relaxation time significantly increased gliding resistance force and energy ($P<.01$), and the difference in energy and force between high- and low-velocity tendon excursions increased with relaxation time ($P=.01$ and $P<.01$). Lastly, without relaxation time, no difference in force and energy was observed ($P=.06$ and $P=.60$), suggesting contact friction.

Interpretation—These findings are consistent with the hypothesis that the mechanics of tendon motion within the carpal tunnel are affected by the integrity of the subsynovial connective tissue. While not tested here, in carpal tunnel syndrome this tissue is known to be the fibrotic, thickened, and less-fluid-permeable. An extrapolation of our findings suggests that these changes in the

---

Corresponding author: Peter C. Amadio, MD, Department of Orthopedic Surgery, Mayo Clinic, 200 First Street SW, Rochester, MN 55905 (pamadio@mayo.edu).

subsynovial connective tissue of carpal tunnel syndrome patients could increase contact friction and carpal tunnel pressure.

Keywords

biomechanics; carpal tunnel syndrome; gliding resistance; SSCT; tendon

1. Introduction

Forceful, high-velocity, and repetitive manual hand tasks can contribute to the onset of carpal tunnel syndrome (CTS) (Atroshi et al., 1999; Barcenilla et al., 2012; Moore et al., 1991; Palmer, 2011; Viera, 2003), a commonly diagnosed neuropathy of the median nerve. Wrist flexion and finger flexion, especially isolated flexion of a single finger (as may occur in typing or other repetitive work), are associated with high tendon gliding resistance (GR) and increased carpal tunnel pressure, which also increases GR (Ettema et al., 2004; Filius et al., 2014; Kociolek et al., 2015; Seradge et al., 1995; Zhao et al., 2011), but little work has been done to elucidate the mechanisms that contribute to tendon GR in the carpal tunnel.

Filius et al. (Filius et al., 2014) and Vanhees et al. (Vanhees et al., 2012) reported that the GR response of the flexor digitorum superficialis (FDS) tendon within the carpal tunnel had an initial "toe" region that was followed by a plateau, in turn followed by an ascending force response. The ascending response has been attributed to stretching of the subsynovial connective tissue (SSCT) (Ettema et al., 2006), a multi-layered structure that surrounds the flexor tendons and median nerve within the carpal tunnel. The SSCT is thought to provide an interface that reduces friction between these structures; however it also restricts tendon motion, especially differential motion between adjacent tendons (Ettema et al., 2006). This assumption is based on previous anatomic research that showed that the FDS tendons within the carpal tunnel, except for the FDS of the little finger, are connected to the SSCT but had no directly interconnecting fibers to other tendons (Leijnse et al., 1997).

The finding of a toe region and plateau is consistent with the response observed in isolated flexor tendon gliding in the zone II-A2 pulley area, suggesting that this behavior is caused by contact friction between tissues (Uchiyama et al., 1997; Uchiyama et al., 1995). It may then be speculated that tendon GR in the carpal tunnel may have a component attributed to contact friction. If the GR could be evaluated by isolating the effect of contact friction and removing other effects (i.e., the SSCT), this speculation could be verified.

Like all living tissues, tissues in the carpal tunnel are infused with an ionic interstitial fluid; interaction of this fluid with the solid phase of these tissues during deformation is a phenomenon known as poroelasticity (Simon, 1992), a behavior which has been demonstrated in other soft tissues such as cartilage (DiSilvestro and Suh, 2001). Poroelasticity of the tendon may become evident when the tendon is pulled through the narrow carpal tunnel and fluid is dispersed out of the tendon as it is deformed, affecting its cross-sectional shape. The poroelastic properties of the tendon, and possibly the SSCT, may also affect GR (Cao and Tang, 2005; Elliott et al., 2003; Sud et al., 2002).

The purpose of this study was to identify factors contributing to tendon GR within the carpal tunnel by sequentially isolating different resistance components related to structural integrity, tendon excursion velocity, and relaxation time allowed between excursions. We hypothesized that the total GR measured during tendon excursion in the carpal tunnel would be the result of a combination of SSCT deformation, (poroelastic) tendon deformation, and contact friction between the flexor tendon and the surrounding tissues (Equation 1) (Figure 1) (Chimich et al., 1992; Clemmer et al., 2010; Lynch et al., 2003; Pioletti et al., 1998; Sud et al., 2002; Zhang, 2005).

$$F_{\text{total gliding resistance}} = F_{\text{SSCT deformation}} + F_{\text{tendon deformation}} + F_{\text{contact friction}} \quad \text{(Equation 1)}$$

To test our hypothesis regarding the role of SSCT, we aimed to compare the total GR to the response after disrupting the SSCT connections to the tendon. We hypothesized that the ascending part of the curve would be eliminated when severing all SSCT connections to the tendon, and that the GR response over a given tendon excursion would then be similar to that observed with tendon excursion in the digits, i.e., a constant GR throughout the excursion, confirming the role of contact friction in the carpal tunnel when the SSCT is not functioning. Lastly, the opportunity to test the isolated tendon GR through the carpal tunnel permits studying the effect of fluid on gliding resistance. We hypothesized that a poroelastic response, if present, would cause a higher GR force and energy for excursions with relaxation time allowed between pulls compared with excursions without relaxation (Cao and Tang, 2005; Chimich et al., 1992; Yin and Elliott, 2004). Allowing no relaxation time between pulls would be expected to nullify any poroelastic effect, and in so doing, the contribution of the contact friction could be confirmed and evaluated. If contact friction were present, it would result in a measurable, nonzero GR which would not be sensitive to the excursion velocity.

2. Materials and Methods

This study was approved by the Mayo Clinic Institutional Review Board. Specimens were obtained from the Mayo Clinic Institutional Anatomical Bequest Program. Eight human cadaver hands (four pairs) were used, with 2 pairs of hands from male subjects. The mean age of the cadaver specimens was 74 years (range 57–83 years). We verified that cadaver specimens did not have a medical history of CTS, upper extremity surgery or fractures of the wrist or hand or disorders to the musculoskeletal system. Specimens were thawed at 5°C for approximately 10 hours before testing.

2.1 Carpal Tunnel Total Gliding Resistance (tendon plus SSCT) Testing

Hands were prepared as previously described (Filius et al., 2014; Vanhees et al., 2012). Briefly, all finger flexor tendons were exposed proximal to the carpal tunnel and the flexor digitorum superficialis (FDS) 2, FDS4 and the flexor digitorum profundus (FDP) 3 tendon were each connected to a 50 g weight. Next, the wrist was mounted onto a jig with the wrist fixed in the neutral position and all fingers fixed with a Kirschner wire in the extended position, except for the middle finger. After determining the physiologic excursion of the FDS3 tendon, the middle finger also was fixed in a fully extended position. The FDS3 and

FDP3 tendons were exposed at the mid palm, but distal to the carpal tunnel and the FDS3 was sharply transected at the level of the metacarpophalangeal joint. The distal end of the FDS3 tendon was connected to a 50-g weight and the proximal end was then connected to a 25 N load cell (MDB-5; Transducer Techniques) (Figure 2).

A stepper motor–driven test actuator controlled the velocity and displacement for each cycle. Four hands were subjected to a displacement velocity of 2 mm/s and four contralateral hands from the same donors were subjected to a velocity of 60 mm/s. Displacement of the stage was monitored with a potentiometer sensor (TR 75; Novotechnik US). Force and displacement data were recorded at a sample rate of 100 Hz for low-velocity tendon excursion (2 mm/s) and 1000 Hz for high-velocity tendon excursion (60 mm/s). The FDS3 tendon was preconditioned by repeating 3 tendon excursions to 5 mm at 2 mm/s. Next, after 15 minutes of relaxation time, the jig was moved 55 mm, resembling FDS3 tendon flexion, which was sufficient to include the 95% CI of the physiologic excursion of the FDS3 tendon, and an additional 5 mm were included for deceleration, so the that the total displacement was 60 mm (Filius et al., 2014; Vanhees et al., 2012). Specimens were tested at room temperature (20°C) and were moistened throughout testing with a sterile saline drip just distal of the carpal tunnel above the FDS3 tendon to prevent structures not sheathed in skin from drying out. A flowchart of experimental conditions is shown in Figure 3.

2.2 Gliding Resistance of Tendon with disrupted SSCT in the Carpal Tunnel

After total gliding resistance of the FDS3 in the carpal tunnel with an intact SSCT had been assessed, the FDS3 was gently pulled from the carpal until it was completely free from the carpal tunnel and all associated SSCT connections had been disrupted. The tendon was then replaced back into its former position in the carpal tunnel. After again preconditioning all hands, regardless of the velocity that had been tested with the SSCT intact, the FDS3 tendons, now with divided SSCT, were tested at tendon excursion velocities of 2 mm/s and 60 mm/s, with and without relaxation time between pulls (Figure 3). These four different conditions (i.e., 2 mm/s without relaxation time, 2 mm/s with relaxation time, 60 mm/s without relaxation time and 60 mm/s with relaxation time) were tested in a random sequence. We felt confident testing in a random order, since we found during pilot testing that when using the same conditions we found similar force-displacement curves repeatedly. Thus the order of testing the different conditions should not have affected the results. The tissue relaxation time was set at 15 minutes between excursions, an adequate period for tissue to reach equilibrium. Combined with the intact SSCT condition tested at two different velocities, a total of six different conditions were tested in this study. The method for evaluating the gliding resistance was as previously described (Filius et al., 2014; Vanhees et al., 2012).

2.3 Data Analysis Rationale

For each of the six conditions, the general shape of the force-displacement curve was grossly assessed. GR force (F) and energy at 100% of the physiologic excursion of the FDS3 tendon were calculated for each tendon excursion as described previously (Filius et al., 2014; Vanhees et al., 2012). The stiffness at 100% of the physiologic excursion for intact SSCT conditions was also calculated where relevant. This was the slope of the linear region at

100% of the physiologic excursion calculated by the forward difference formula (Equation 2).

$$\text{Slope} = (F_2 - F_1)/(X_2 - X_1) \quad \text{(Equation 2)}$$

SSCT deformation—To determine the contribution of the SSCT to GR, we first assessed the GR with intact SSCT. Next we measured the GR with divided SSCT after relaxation time and compared these GR curves, matching tested velocities within the same hand with intact and with divided SSCT. Because all SSCT connections were severed in the second phase of the experiment, we expected the difference to be the force component $F_{\text{SSCT deformation}}$ in the model. Figure 4 provides a representative example of the force-displacement response with intact and with divided SSCT. This assessment was done for four hands at the low-velocity and four contralateral hands at the high-velocity tendon excursion.

Poroelastic Properties—The contribution of tendon deformation as it contacts carpal tunnel tissues was evaluated by evaluating GR response of a tendon separated from the SSCT passing through the carpal tunnel. Two sequential excursions with and without relaxations time between tests were compared. It was thought that a poroelastic effect would be supported if the difference between subsequent excursions was amplified with higher tendon excursion velocities and with relaxation time between excursions.

Contact Friction—Allowing no relaxation time between pulls was expected to nullify any poroelastic effect, and in so doing, the contribution of the contact friction could be confirmed and evaluated. If the contact friction effect was present, we anticipated that it would result in a measurable, nonzero GR and that this value would not be sensitive to the excursion velocity.

2.4 Statistical Analysis

Statistical analyses were performed using the Statistical Package for Social Science software version 17.0 (SPSS, Chicago (IL)). To evaluate the contribution of SSCT to gliding resistance at different excursion velocities, a two-way ANOVA was performed on the force and energy at 100% excursion with factors of SSCT condition (intact and divided) and velocity (2 mm/s and 60 mm/s). When analyzing the gliding resistance of the FDS3 tendon dissociated from the SSCT the paired-*t* test was used. *P* values <.05 were considered significant.

3. Results

The mean physiologic excursion of the FDS3 tendon was 18.4 mm (range, 16.4–21.3 mm).

Testing with the SSCT Intact

A typical force-displacement curve with the SSCT intact included a toe region, a plateau, and a liner slope (Figure 4). The two-way ANOVA analysis showed there was a significant

difference in force at 100% excursion between the intact and severed SSCT conditions (P = 0.005) and between the two velocities (P = 0.039), but there was no significant interaction effect (P = 0.176). The two-way ANOVA analysis showed there was a significant difference in energy at 100% excursion between the intact and severed SSCT conditions (P=0.007) and between the two velocities (P = 0.012), but there was no significant interaction effect (P = 0.204) (Table 1). Upon isolating the contribution of SSCT stretching to the GR, by taking the difference between the GR with SSCT intact and that with the SSCT disrupted, we found a monotonically ascending curve remained (Figure 4).

At the beginning of the FDS3 tendon excursion, SSCT stretching contributed 40% to the total GR; at the end of the physiologic excursion, SSCT stretching contributed nearly 100% to the GR (Figure 5).

Testing with the SSCT Divided

Next, we analyzed the poroelastic properties of the tendon. When comparing GR with and without relaxation time, GR force and energy were significantly different (all $P<.01$) (Table 2). The absolute difference in GR force and energy between pulls with and without relaxation time was amplified more at the higher tendon excursion velocity compared to the low-velocity tendon excursion.

Lastly, we analyzed contact friction. With no relaxation allowed to take place before testing, GR was measured to be 48 mN with low-velocity tendon excursion and 55 mN with high-velocity tendon excursion, which was not significantly different (P=0.06). GR energy was measured to be 752 mN and 772 mN at low- and high-velocity tendon excursion, respectively, which also was not significantly different (P=0.60) (Table 2).

4. Discussion

CTS is often associated with occupations that involve high-velocity repetitive hand and wrist motions and is characterized by increased carpal tunnel pressure. Both increased pressure and high-velocity tendon motion result in increased GR, which suggests that high GR is related to CTS (Filius et al., 2014; Kociolek et al., 2015; Tat et al., 2013; Zhao et al., 2011). A good understanding of GR in the carpal tunnel is, therefore, important to better understand the pathology of CTS. Although various studies have evaluated the GR and frictional work of the flexor tendon in the carpal tunnel during various motions and hand-wrist positions, the mechanisms involved in GR have not been delineated. The significant difference in GR observed between intact and severed SSCT conditions indicates the prominent contribution of SSCT stretching to the total GR. The significant effect of relaxation time and sensitivity to velocity on the GR when evaluating tendon excursions with the SSCT severed fits with our hypothesis for the presence of a poroelastic effect. Furthermore, that we observed a GR contribution with this poroelastic effect nullified that was not sensitive to tendon velocity fits with our hypothesis that contact friction contributes to the total resistance as well.

An increase in GR force, energy, and stiffness due to SSCT stretching was observed at larger excursions and higher tendon excursion velocities. Previous studies have speculated that the ascending part of the GR curve was an isolated result of SSCT stretching (Filius et al., 2014;

Morizaki et al., 2012; Osamura et al., 2007). This hypothesis is further confirmed based on our findings, which showed that after tendon pull out there was a static GR curve after an initial toe region, and that the resistance force was significantly different than with the intact SSCT condition. SSCT characteristics correspond to those of viscoelastic materials, providing support for the idea that SSCT is a viscoelastic tissue (Clemmer et al., 2010; Lynch et al., 2003; McElhaney, 1966; Zhang, 2005). In an ex vivo experiment with SSCT of patients with CTS, increased stiffening of the SSCT and SSCT embrittlement were identified (Osamura et al., 2007). If the same mechanism applies to the SSCT at high-velocity tendon excursion, it may explain why high-velocity tendon excursion is a risk factor for CTS, e.g. such motions might lead to damage to the stiffened SSCT, subsequent fibrosis and further stiffening of the SSCT, and a vicious cycle of injury and fibrosis that would ultimately affect tendon function and carpal tunnel pressure, as increasing tendon loading would be needed to effect finger motion.

After disrupting the connection between the SSCT fibers and the FDS3 tendon, we observed a static GR curve after an initial toe region. The height of this curve was determined by relaxation time and tendon excursion velocity. GR increased with relaxation time between pulls, and increasing tendon excursion velocity amplified this effect. This type of tissue response to the different test conditions is typical of poroelastic materials and we hypothesize that it is the result of cross-sectional tendon deformation as the tendon is moved through the carpal tunnel (Cao and Tang, 2005; Noailly et al., 2008).

Since GR was still evident, even without relaxation time between tendon excursion cycles, we believe it was caused by contact friction with surrounding tissues. This low but constant resistance has been identified in other flexor tendon excursion experiments that do not involve the SSCT (Uchiyama et al., 1997; Uchiyama et al., 1995). Whether the absolute GR is equal to that of the intrasynovial flexor digitorum profundus tendon GR through the A2-pulley could not be demonstrated here, since the different loads and test set up preclude direct comparison of the results (Moriya et al., 2011; Uchiyama et al., 1997).

This study was done in cadaver hands. Therefore the absolute results cannot be translated directly to the in vivo situation. In vivo internal fluids are made continuously by tissue, and the skin protects against dehydration. We had to moisten our cadaver hands with sterile saline, which has different rheological properties than human interstitial fluid. Although saline is a standard means of attempting to simulate physiologic conditions when testing tendons, saline can be absorbed more actively compared with normal internal fluids (Chimich et al., 1992; Vanhees et al., 2012). Therefore, the moistening may have led to a nonphysiologic increase of GR. However, the mechanisms will not be different, and therefore we believe that the results reported here can be used to better understand the mechanisms involved in gliding resistance within the carpal tunnel. Also, it must be noted that the sample size in this study was small (four pairs of hands). However even with this small sample size, we were able to detect the large differences resulting from severing the SSCT.

In summary, SSCT stretching, contact friction and poroelastic properties of the tendon and SSCT all affect GR. By dividing the GR into different components we can better study the

impact of GR on CTS and this create insights on the pathomechanism of CTS. These studies, in turn, may lead to new insights about the physiology of CTS and, hopefully, its treatment.

Acknowledgments

Abbreviations

CTS	carpal tunnel syndrome
F	force
FDS3	flexor digitorum superficialis tendon of the middle finger
GR	gliding resistance
SSCT	subsynovial connective tissue

References

Atroshi I, Gummesson C, Johnsson R, Ornstein E, Ranstam J, Rosen I. Prevalence of carpal tunnel syndrome in a general population. JAMA. 1999; 282:153–158. [PubMed: 10411196]

Barcenilla A, March LM, Chen JS, Sambrook PN. Carpal tunnel syndrome and its relationship to occupation: a meta-analysis. Rheumatology. 2012; 51:250–261. [PubMed: 21586523]

Cao Y, Tang JB. Investigation of resistance of digital subcutaneous edema to gliding of the flexor tendon: an in vitro study. J Hand Surg Am. 2005; 30:1248–1254. [PubMed: 16344184]

Chimich D, Shrive N, Frank C, Marchuk L, Bray R. Water content alters viscoelastic behaviour of the normal adolescent rabbit medial collateral ligament. Journal of biomechanics. 1992; 25:831–837. [PubMed: 1639827]

Clemmer J, Liao J, Davis D, Horstemeyer MF, Williams LN. A mechanistic study for strain rate sensitivity of rabbit patellar tendon. Journal of biomechanics. 2010; 43:2785–2791. [PubMed: 20678772]

DiSilvestro MR, Suh JK. A cross-validation of the biphasic poroviscoelastic model of articular cartilage in unconfined compression, indentation, and confined compression. Journal of biomechanics. 2001; 34:519–525. [PubMed: 11266676]

Elliott DM, Robinson PS, Gimbel JA, Sarver JJ, Abboud JA, Iozzo RV, Soslowsky LJ. Effect of altered matrix proteins on quasilinear viscoelastic properties in transgenic mouse tail tendons. Annals of Biomedical Engineering. 2003; 31:599–605. [PubMed: 12757203]

Ettema AM, Amadio PC, Zhao C, Wold LE, An KN. A histological and immunohistochemical study of the subsynovial connective tissue in idiopathic carpal tunnel syndrome. J Bone Joint Surg Am. 2004; 86-A:1458–1466. [PubMed: 15252093]

Ettema AM, Zhao C, An KN, Amadio PC. Comparative anatomy of the subsynovial connective tissue in the carpal tunnel of the rat, rabbit, dog, baboon, and human. Hand. 2006; 1:78–84. [PubMed: 18780029]

Filius A, Thoreson AR, Yang TH, Vanhees M, An KN, Zhao C, Amadio PC. The effect of low- and high-velocity tendon excursion on the mechanical properties of human cadaver subsynovial connective tissue. Journal of orthopaedic research : official publication of the Orthopaedic Research Society. 2014; 32:123–128. [PubMed: 24038298]

Kociolek AM, Tat J, Keir PJ. Biomechanical risk factors and flexor tendon frictional work in the cadaveric carpal tunnel. Journal of biomechanics. 2015; 48:449–455. [PubMed: 25553671]

Leijnse JN, Walbeehm ET, Sonneveld GJ, Hovius SE, Kauer JM. Connections between the tendons of the musculus flexor digitorum profundus involving the synovial sheaths in the carpal tunnel. Acta Anat (Basel). 1997; 160:112–122. [PubMed: 9673709]

Lynch HA, Johannessen W, Wu JP, Jawa A, Elliott DM. Effect of fiber orientation and strain rate on the nonlinear uniaxial tensile material properties of tendon. Journal of biomechanical engineering. 2003; 125:726–731. [PubMed: 14618932]

McElhaney JH. Dynamic response of bone and muscle tissue. Journal of applied physiology. 1966; 21:1231–1236. [PubMed: 5916656]

Moore A, Wells R, Ranney D. Quantifying exposure in occupational manual tasks with cumulative trauma disorder potential. Ergonomics. 1991; 34:1433–1453. [PubMed: 1800109]

Moriya T, Chikenji T, Thoreson AR, Zhao C, An KN, Amadio PC. Effects of different temperatures, velocities and loads on the gliding resistance of flexor digitorum profundus tendons in a human cadaver model. Journal of biomechanics. 2011; 44:1414–1416. [PubMed: 21276970]

Morizaki Y, Vanhees M, Thoreson AR, Larson D, Zhao C, An KN, Amadio PC. The response of the rabbit subsynovial connective tissue to a stress-relaxation test. Journal of orthopaedic research : official publication of the Orthopaedic Research Society. 2012; 30:443–447. [PubMed: 21898581]

Noailly J, Van Oosterwyck H, Wilson W, Quinn TM, Ito K. A poroviscoelastic description of fibrin gels. Journal of biomechanics. 2008; 41:3265–3269. [PubMed: 18930461]

Osamura N, Zhao C, Zobitz ME, An KN, Amadio PC. Evaluation of the material properties of the subsynovial connective tissue in carpal tunnel syndrome. Clinical biomechanics. 2007; 22:999–1003. [PubMed: 17822815]

Palmer KT. Carpal tunnel syndrome: the role of occupational factors. Best practice & research. Clinical rheumatology. 2011; 25:15–29. [PubMed: 21663847]

Pioletti DP, Rakotomanana LR, Benvenuti JF, Leyvraz PF. Viscoelastic constitutive law in large deformations: application to human knee ligaments and tendons. Journal of biomechanics. 1998; 31:753–757. [PubMed: 9796676]

Seradge H, Jia YC, Owens W. In vivo measurement of carpal tunnel pressure in the functioning hand. J Hand Surg Am. 1995; 20:855–859. [PubMed: 8522756]

Simon BR. Multiphase poroelastic finite element models for soft tissue structures. Apll Mech Rev. 1992; 45:191–218.

Sud V, Tucci MA, Freeland AE, Smith WT, Grinspun K. Absorptive properties of synovium harvested from the carpal tunnel. Microsurgery. 2002; 22:316–319. [PubMed: 12404351]

Tat J, Kociolek AM, Keir PJ. Repetitive differential finger motion increases shear strain between the flexor tendon and subsynovial connective tissue. Journal of orthopaedic research : official publication of the Orthopaedic Research Society. 2013; 31:1533–1539. [PubMed: 23729391]

Uchiyama S, Amadio PC, Coert JH, Berglund LJ, An KN. Gliding resistance of extrasynovial and intrasynovial tendons through the A2 pulley. J Bone Joint Surg Am. 1997; 79:219–224. [PubMed: 9052543]

Uchiyama S, Coert JH, Berglund L, Amadio PC, An KN. Method for the measurement of friction between tendon and pulley. Journal of orthopaedic research : official publication of the Orthopaedic Research Society. 1995; 13:83–89. [PubMed: 7853108]

Vanhees M, Morizaki Y, Thoreson AR, Larson D, Zhao C, An KN, Amadio PC. The effect of displacement on the mechanical properties of human cadaver subsynovial connective tissue. Journal of orthopaedic research : official publication of the Orthopaedic Research Society. 2012; 30:1732–1737. [PubMed: 22573580]

Viera AJ. Management of carpal tunnel syndrome. American family physician. 2003; 68:265–272. [PubMed: 12892346]

Yin L, Elliott DM. A biphasic and transversely isotropic mechanical model for tendon: application to mouse tail fascicles in uniaxial tension. Journal of biomechanics. 2004; 37:907–916. [PubMed: 15111078]

Zhang G. Evaluating the viscoelastic properties of biological tissues in a new way. J Musculoskelet Neuronal Interact. 2005; 5:85–90. [PubMed: 15788874]

Zhao C, Ettema AM, Berglund LJ, An KN, Amadio PC. Gliding resistance of flexor tendon associated with carpal tunnel pressure: a biomechanical cadaver study. Journal of orthopaedic research: official publication of the Orthopaedic Research Society. 2011; 29:58–61. [PubMed: 20661935]

Highlights

- Subsynovial connective tissue stiffness is proportional to tendon gliding velocity.

- Subsynovial connective tissue stretch, poroelasticity and friction resist gliding.

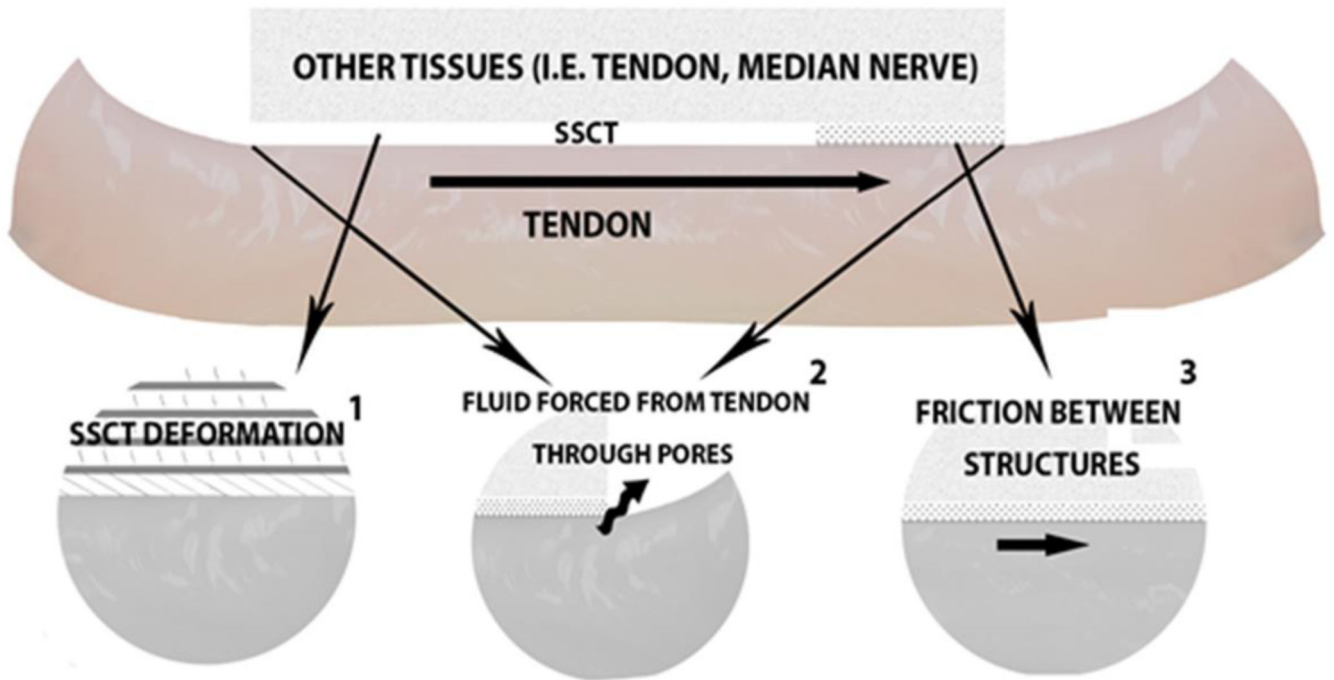- Carpal tunnel syndrome induced changes could further increase gliding resistance.

Figure 1.
Carpal Tunnel Components Thought to Have a Role in Gliding Resistance. Resistance may be affected by 1) subsynovial connective tissue (SSCT) deformation, 2) tendon deformation (poroelasticity), and 3) residual contact friction.
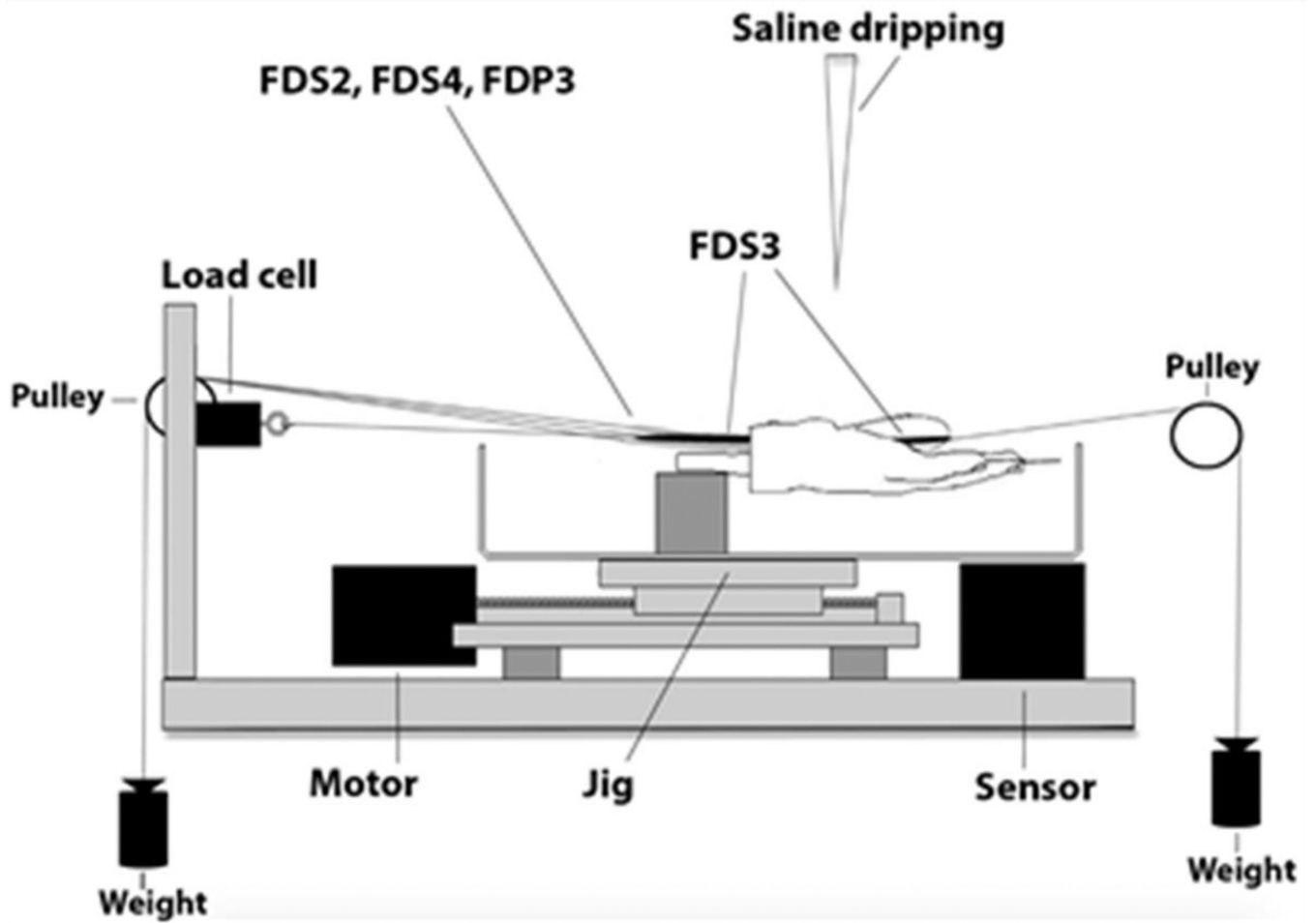
Figure 2.
Experimental Setup. FDP, indicates flexor digitorum profundus; FDS, flexor digitorum superficialis. (Adapted from Filius et al. (Filius et al., 2014). Used with permission.)
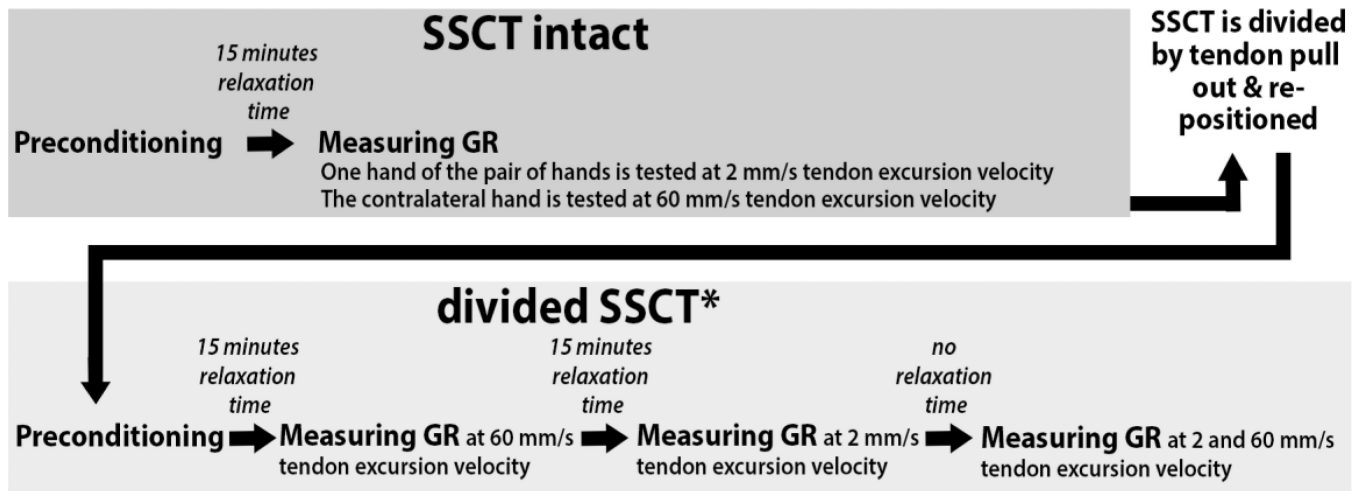
Figure 3.
Flow Diagram of the Mechanical Testing Protocol. For the not-intact subsynovial connective tissue (SSCT) experiments, the order of testing (e.g., 2 or 60 mm/s, with or without relaxation time) was chosen randomly.
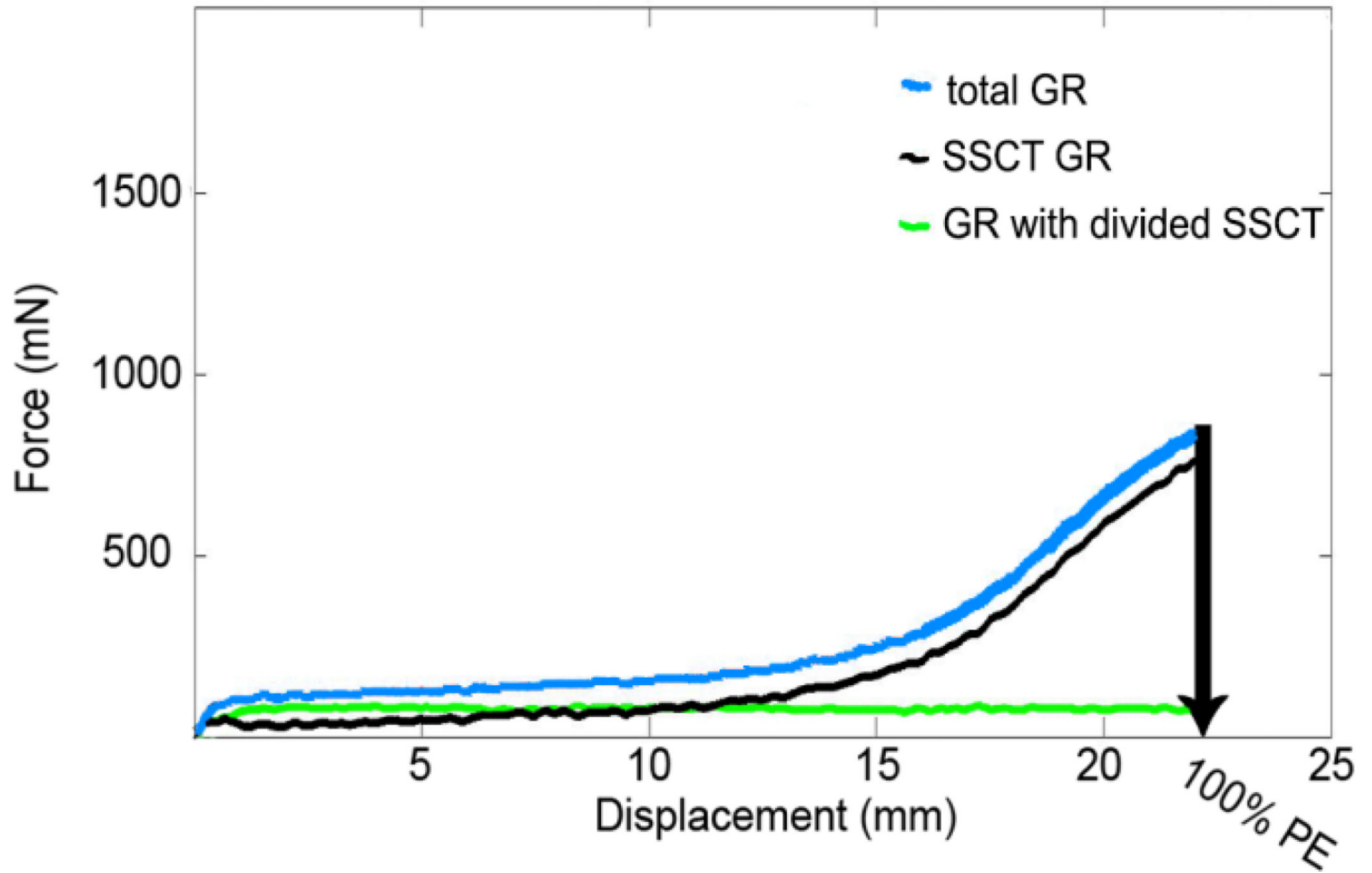
Figure 4.
A representative example of the FDS3 tendon force-displacement curve of the total GR at low-velocity excursion within a cadaver hand with SSCT intact (blue) and SSCT divided (green) and the SSCT force-displacement curve (black), Abbreviations: PE; physiological excursion of the FDS3 tendon.
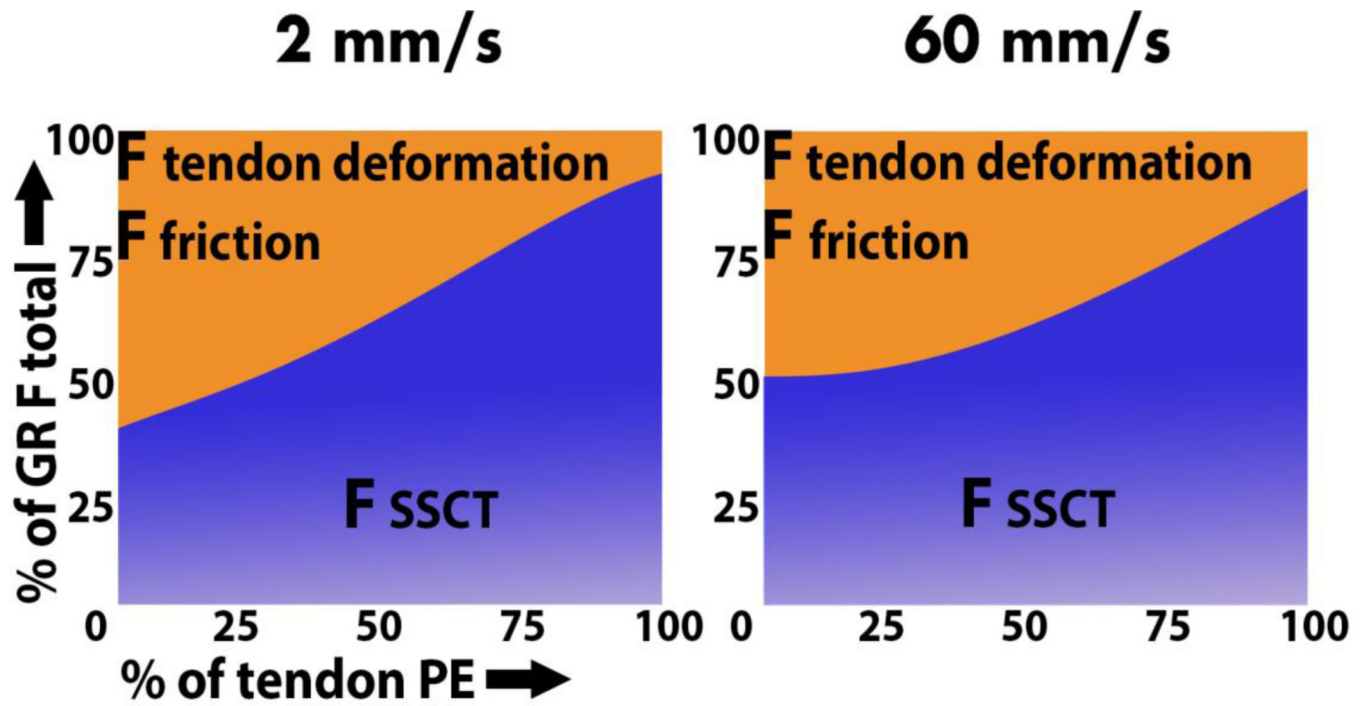
Figure 5.
$F_{SSCT\ deformation}$ as portion of the total GR force. A. Excursion velocity, 2 mm/s. B. Excursion velocity, 60 mm/s. F indicates force; GR, gliding resistance; PE, physiologic excursion; SSCT, subsynovial connective tissue.

Table 1

Contribution of Subsynovial Connective Tissue to Gliding Resistance at 100% of the Physiologic Excursion of the Flexor Digitorum Superficialis Tendon of the middle finger[a].

	Excursion Speed	
Characteristics	**Slow (N=4)**	**Fast (N=4)**
SSCT Intact		
Force, mN	780 (686–1,149)	1,387 (1,068–3,050)
Energy, μJ	5,438 (3,546–5,929)	10,534 (7,770–23,789)
Stiffness, mN/mm	136 (75–225)	213 (161–496)
SSCT Divided		
Force, mN	73 (37–109)	266 (170–407)
Energy, μJ	1,337 (1,004–2,191)	4,015 (3,114–6,882)
Stiffness, mN/mm	N/A	N/A
Intact - Divided		
Force, mN	721 (577–1,084)	1,145 (852–2,643)
Energy, μJ	3,667 (2,542–4,607)	6,518 (4,656–16,907)
Stiffness, mN/mm	144 (72–219)	215 (164–519)

Abbreviations: SSCT, subsynovial connective tissue; fast, 60 mm/s; FDS3; slow, 2 mm/s.

[a]Data are shown as median (range).

Table 2

Contribution of Poroelasticity to Gliding Resistance[a].

| Characteristic | With Relaxation | | | Without Relaxation | | | P Value[b] | |
	Slow	Fast	P Value	Slow	Fast	P Value	Slow	Fast
Force, mN	69 (25)	279 (146)	.01	48 (16)	55 (16)	.06	<.01	<.01
Energy, μJ	1,328 (472)	4,356 (346)	<.01	752 (276)	772 (220)	.60	<.01	<.01

Abbreviations: fast, 60 mm/s excursion speed; slow, 2 mm/s excursion speed.

[a]Data were obtained using 8 cadaver hands (four pairs). Data are shown as mean (SD).

[b]Comparison of outcomes with and without relaxation, using the same excursion velocities.